EUROPEAN ORGANIZATION FOR NUCLEAR RESEARCH

CERN-EP/89-169
December 19th, 1989

A Precise Determination of the Number of Families with Light Neutrinos and of the Z Boson Partial Widths.

19 December 1989

The ALEPH Collaboration

D. Decamp, B. Deschizeaux, J.-P. Lees, M.-N. Minard

Laboratoire de Physique des Particules (LAPP), IN²P³-CNRS, 74019 Annecy-le-Vieux Cedex, France

J.M. Crespo, M. Delfino, E. Fernandes[1], M. Martines, R. Miquel, Ll.M. Mir, S. Orteu, A. Pacheco, J.A. Perlas, E. Tubau

Laboratorio de Fisica de Altas Energias, Universidad Autonoma de Barcelona, 08193 Bellaterra (Barcelona), Spain[9]

M.G. Catanesi, M. de Palma, A. Farilla, G. Iaselli, G. Maggi, S. Natali, S. Nuzzo, A. Ranieri, G. Raso, F. Romano, F. Ruggieri, G. Selvaggi, L. Silvestris, P. Tempesta, G. Zito

INFN Sezione di Bari e Dipartimento di Fisica dell' Università, 70126 Bari, Italy

H. Hu, D. Huang, J. Lin, T. Ruan, T. Wang, W. Wu, Y. Xie, D. Xu, R. Xu, J. Zhang, W. Zhao

Institute of High-Energy Physics, Academia Sinica, Beijing, The People's Republic of China[10]

H. Albrecht[2], W.B. Atwood[3], F. Bird, E. Blucher, T.H. Burnett[4], T. Charity, H. Drevermann, Ll. Garrido, C. Grab, R. Hagelberg, S. Haywood, B. Jost, M. Kasemann, G. Kellner, J. Knobloch, A. Lacourt, I. Lehraus, T. Lohse, D. Lüke[2], A. Marchioro, P. Mato, J. May, A. Minten, A. Miotto, P. Palazzi, M. Pepe-Altarelli, F. Ranjard, A. Roth, J. Rothberg[4], H. Rotscheidt, W. von Rüden, R. St.Denis, D. Schlatter, M. Takashima, M. Talby, H. Taureg, W. Tejessy, H. Wachsmuth, S. Wheeler, W. Wiedenmann, W. Witzeling, J. Wotschack

European Laboratory for Particle Physics (CERN), 1211 Geneva 23, Switzerland

Z. Ajaltouni, M. Bardadin-Otwinowska, A. Falvard, P. Gay, P. Henrard, J. Jousset, B. Michel, J-C. Montret, D. Pallin, P. Perret, J. Proriol, F. Prulhière

Laboratoire de Physique Corpusculaire, Université Blaise Pascal, IN²P³-CNRS, Clermont-Ferrand, 63177 Aubière, France

J.D. Hansen, J.R. Hansen, P.H. Hansen, R. Mø llerud, G. Petersen

Niels Bohr Institute, 2100 Copenhagen, Danmark[11]

E. Simopoulou, A. Vayaki

Nuclear Research Center Demokritos (NRCD), Athens, Greece

J. Badier, A. Blondel, G. Bonneaud, J. Bourotte, F. Braems, J.C. Brient, M.A. Ciocci, G. Fouque, R. Guirlet, A. Rougé, M. Rumpf, R. Tanaka, H. Videau, I. Videau[1]

Laboratoire de Physique Nucléaire et des Hautes Energies, Ecole Polytechnique, IN²P³-CNRS, 91128 Palaiseau Cedex, France

(Submitted to Physics Letters)

D.J. Candlin

Department of Physics, University of Edinburgh, Edinburgh EH9 3JZ, United Kingdom[12]

A. Conti, G. Parrini

Dipartimento di Fisica, Università di Firenze, INFN Sezione di Firenze, 50125 Firenze, Italy

M. Corden, C. Georgiopoulos, J.H. Goldman, M. Ikeda, J. Lannutti, D. Levinthal[17], M. Mermikides, L. Sawyer, G. Stimpfl

Supercomputer Computations Research Institute and Dept. of Physics, Florida State University, Tallahassee FL 32306, USA[14,15,16]

A. Antonelli, R. Baldini, G. Bencivenni, G. Bologna[5], F. Bossi, P. Campana, G. Capon, V. Chiarella, G. De Ninno, B. D'Ettorre-Piazzoli[6], G. Felici, P. Laurelli, G. Mannocchi[6], F. Murtas, G.P. Murtas, G. Nicoletti, P. Picchi[5], P. Zografou

Laboratori Nazionali dell'INFN (LNF-INFN), 00044 Frascati, Italy

B. Altoon, O. Boyle, A.W. Halley, I. ten Have, J.L. Hearns, I.S. Hughes, J.G. Lynch, W.T. Morton, C. Raine, J.M. Scarr, K. Smith[1], A.S. Thompson

Department of Physics and Astronomy, University of Glasgow, Glasgow G12 8QQ, United Kingdom[12]

B. Brandl, O. Braun, R. Geiges, C. Geweniger[1], P. Hanke, V. Hepp, E.E. Kluge, Y. Maumary, M. Panter, A. Putzer, B. Rensch, A. Stahl, K. Tittel, M. Wunsch

Institut für Hochenergiephysik, Universität Heidelberg, 6900 Heidelberg, Fed. Rep. of Germany[18]

A.T. Belk, R. Beuselinck, D.M. Binnie, W. Cameron[1], M. Cattaneo, P.J. Dornan, S. Dugeay, R.W. Forty, A.M. Greene, J.F. Hassard, S.J. Patton, J.K. Sedgbeer, G. Taylor, I.R. Tomalin, A.G. Wright

Department of Physics, Imperial College, London SW7 2BZ, United Kingdom[12]

P. Girtler, D. Kuhn, G. Rudolph

Institut für Experimentalphysik, Universität Innsbruck, 6020 Innsbruck, Austria[20]

C.K. Bowdery[1], T.J. Brodbeck, A.J. Finch, F. Foster, G. Hughes, N.R. Keemer, M. Nuttall, B.S. Rowlingson, T. Sloan, S.W. Snow

Department of Physics, University of Lancaster, Lancaster LA1 4YB, United Kingdom[12]

T. Barczewski, L.A.T. Bauerdick, K. Kleinknecht[1], B. Renk, S. Roehn, H.-G. Sander, M. Schmelling, F. Steeg

Institut für Physik, Universität Mainz, 6500 Mainz, Fed. Rep. of Germany [18]

J-P. Albanese, J-J. Aubert, C. Benchouk, A. Bonissent, D. Courvoisier, F. Etienne, E. Matsinos, S. Papalexiou, P. Payre, B. Pietrzyk[1], Z. Qian

Centre de Physique des Particules, Faculté des Sciences de Luminy, IN²P³-CNRS, 13288 Marseille, France

W. Blum, P. Cattaneo, G. Cowan, B. Dehning, H. Dietl, M. Fernandez-Bosman, D. Hauff, A. Jahn, E. Lange, G. Lütjens, G. Lutz, W. Männer, H-G. Moser, Y. Pan, R. Richter, A.S. Schwarz, R. Settles, U. Stiegler, U. Stierlin, J. Thomas, G. Waltermann

Max-Planck-Institut für Physik und Astrophysik, Werner-Heisenberg-Institut für Physik, 8000 München, Fed. Rep. of Germany[18]

V. Bertin, G. de Bouard, J. Boucrot, O. Callot, X. Chen, A. Cordier, M. Davier, G. Ganis, J.-F. Grivaz, Ph. Heusse, P. Janot, V. Journé, D.W. Kim, J. Lefrançois, A.-M. Lutz, J.-J. Veillet, F. Zomer

Laboratoire de l'Accéléateur Linéaire, Université de Paris-Sud, IN²P³-CNRS, 91405 Orsay Cedex, France

S.R. Amendolia, G. Bagliesi, G. Batignani, L. Bosisio, U. Bottigli, C. Bradaschia, I. Ferrante, F. Fidecaro, L. Foà[1], E. Focardi, F. Forti, A. Giassi, M.A. Giorgi, F. Ligabue, A. Lusiani, E.B. Mannelli, P.S. Marrocchesi, A. Messineo, F. Palla, G. Sanguinetti, S. Scapellato, J. Steinberger, R. Tenchini, G. Tonelli, G. Triggiani

Dipartimento di Fisica dell'Università, INFN Sezione di Pisa, e Scuola Normale Superiore,56010 Pisa, Italy

J.M. Carter, M.G. Green, P.V. March, T. Medcalf, M.R. Saich, J.A. Strong[1], R.M. Thomas, T. Wildish
Department of Physics, Royal Holloway & Bedford New College, University of London, Surrey TW20 OEX, United Kingdom[12]

D.R. Botterill, R.W. Clifft, T.R. Edgecock, M. Edwards, S.M. Fisher, J. Harvey, T.J. Jones, P.R. Norton, D.P. Salmon, J.C. Thompson
Particle Physics Dept., Rutherford Appleton Laboratory, Chilton, Didcot, OXON OX11 OQX, United Kingdom[12]

E. Aubourg, B. Bloch-Devaux, P. Colas, C. Klopfenstein, E. Lançon, E. Locci, S. Loucatos, L. Mirabito, E. Monnier, P. Perez, F. Perrier, J. Rander, J.-F. Renardy, A. Roussarie, J.-P. Schuller
Département de Physique des Particules Élémentaires, CEN-Saclay, 91191 Gif-sur-Yvette Cedex, France[19]

J.G. Ashman, C.N. Booth, F. Combley, M. Dinsdale, J. Martin, D. Parker, L.F. Thompson
Department of Physics, University of Sheffield, Sheffield S3 7RH, United Kingdom[12]

S. Brandt, H. Burkhardt, C. Grupen, H. Meinhard, E. Neugebauer, U. Schäfer, H. Seywerd
Fachbereich Physik, Universität Siegen, 5900 Siegen, Fed. Rep. of Germany[18]

B. Gobbo, F. Liello, E. Milotti, F. Ragusa[7], L. Rolandi[1]
Dipartimento di Fisica, Università di Trieste e INFN Sesione di Trieste, 34127 Trieste, Italy

L. Bellantoni, J.F. Boudreau, D. Cinabro, J.S. Conway, D.F. Cowen, Z. Feng, J.L. Harton, J. Hilgart, R.C. Jared[8], R.P. Johnson, B.W. LeClaire, Y.B. Pan, T. Parker, J.R. Pater, Y. Saadi, V. Sharma, J.A. Wear, F.V. Weber, Sau Lan Wu, S.T. Xue, G. Zobernig
Department of Physics, University of Wisconsin, Madison, WI 53706, USA [13]

(Submitted to Phys. Lett. B)

---

[1] Now at CERN.
[2] Permanent address: DESY, Hamburg, Fed. Rep. of Germany.
[3] On leave of absence from SLAC, Stanford, CA 94309, USA.
[4] On leave of absence from University of Washington, Seattle, WA 98195, USA.
[5] Also Istituto di Fisica Generale, Università di Torino, Torino, Italy.
[6] Also Istituto di Cosmo-Geofisica del C.N.R., Torino, Italy.
[7] Now at INFN Milano.
[8] Permanent address: LBL, Berkeley, CA 94720, USA.
[9] Supported by CAICYT, Spain.
[10] Supported by the National Science Foundation of China.
[11] Supported by the Danish Natural Science Research Council.
[12] Supported by the UK Science and Engineering Research Council.
[13] Supported by the US Department of Energy, contract DE-AC02-76ER00881.
[14] Supported by the US Department of Energy, contract DE-FG05-87ER40319.
[15] Supported by the NSF, contract PHY-8451274.
[16] Supported by the US Department of Energy, contract DE-FC0S-85ER250000.
[17] Supported by SLOAN fellowship, contract BR 2703.
[18] Supported by the Bundesministerium für Forschung und Technologie, Fed. Rep. of Germany.
[19] Supported by the Institut de Recherche Fondamentale du C.E.A..
[20] Supported by Fonds zur Förderung der wissenschaftlichen Forschung, Austria.

Abstract

More extensive and precise results are reported on the parameters of Z decay. On the basis of 20 000 Z decays collected with the ALEPH detector at LEP we find:

$$M_z = 91.182 \pm 0.026 \text{ (exp)} \pm 0.030 \text{ (beam) GeV}$$
$$\Gamma_z = 2.541 \pm 0.056 \text{ GeV}$$
and $$\sigma^o_{had} = 41.4 \pm 0.8 \text{ nb.}$$

The partial widths for the hadronic and leptonic channels are:

$$\Gamma_{had} = 1804 \pm 44 \text{ MeV}$$
$$\Gamma_{e^+e^-} = 82.1 \pm 3.4 \text{ MeV}$$
$$\Gamma_{\mu^+\mu^-} = 87.9 \pm 6.0 \text{ MeV}$$
and $$\Gamma_{\tau^+\tau^-} = 86.1 \pm 5.6 \text{ MeV,}$$

in good agreement with the standard model. On the basis of the average leptonic width $\Gamma_{l^+l^-} = 83.9 \pm 2.2$ MeV, the effective weak mixing angle is found to be $\sin^2\theta_w(M_z) = 0.231 \pm 0.008$.

Using the partial widths calculated in the standard model, the number of light neutrino families is $N_\nu = 3.01 \pm 0.15(\text{exp}) \pm 0.05$ (theo).

1. Introduction

With the start-up of LEP, one of the interesting questions which could be addressed was that of the number of neutrino species into which the Z decays, not by the direct observation of the neutrinos, but by a precise measurement of the Z width, or of the cross-section at the Z peak. The latter is statistically more powerful, but systematically more demanding because it requires precise knowledge of the absolute luminosity and of the Z decay detection efficiency. Several results based on the cross-section have been reported recently [1-5] and are in agreement with three neutrino families, however, the most precise of these [5] is only $2^1/_2$ standard deviations away from four families. We therefore believe it useful to report the continuation of our work, based on a six-fold statistical increase in the data sample. The analysis has remained basically the same, but the detector has continuously improved and our understanding of the systematic errors has progressed. In addition to the number of neutrino families N_ν, new results for the Z mass and line shape, as well as the leptonic branching ratios are given. For a brief description of the detector, we refer to ref. 5. A more detailed description is in preparation [6].

2. Event triggers

Two independent triggers are used in this analysis: i) a basic trigger based on the electromagnetic calorimeter (ECAL), which requires a total energy of 6.5 GeV in the ECAL barrel, 3.8 GeV in either ECAL end-cap, or 1.6 GeV in both end-caps; ii) a penetrating-charged-particle trigger, which requires that at least 5 inner tracking chamber (ITC) wire planes and at least 4 hadron calorimeter (HCAL) double planes give signals in the same azimuthal region.

3. Z Event selection and efficiency

Events are selected in two independent ways, one based on calorimetric energy, the other on charged tracks. Both require the basic trigger; the other trigger is used exclusively to measure the trigger efficiency.

The calorimetric selection requires a minimum total electromagnetic and hadronic energy of at least 20 GeV. In addition it is required that at least 6 GeV of this energy be in the ECAL barrel or 1.5 GeV in each of the ECAL end-caps. If there are at least 5 time projection chamber (TPC) tracks (95% of the events) there are no further requirements. For events with 1 to 4 tracks, additional cuts are imposed to eliminate $e^+ e^-$ and $\mu^+ \mu^-$ final states. Bhabhas are rejected on the basis of their characteristic tight energy clusters in the electromagnetic calorimeter. To eliminate muonic decays, events are rejected if there are exactly two tracks, each with associated hits (4 or more strips in the 10 outer layers) in HCAL. For events with no tracks at all, two additional cuts are applied to

eliminate cosmic rays: a time window of ± 350 nsec based on timing in ECAL, and a requirement of at least two clusters of 3 GeV each in ECAL. This selection leaves 18 654 events: 16 930 with 5 or more tracks, 872 with 1 to 4 tracks, and 852 with no tracks. This latter class includes 804 events with the TPC turned off. All events with less than 5 tracks were visually inspected; 121 events were identified as Bhabha events in which one or both electrons are in the cracks of ECAL but the energy could be seen in HCAL, 14 events are classified as beam gas interactions, 3 as muon pairs, and 92 could not be identified, so that 46 with an error of ± 46 were included in the final event sample. As a check, in the visual inspection, $\tau^+\tau^-$ decays were identified. Almost all $\tau^+\tau^-$ events should appear in the 1-4 track category. On the basis of the branching ratio $\Gamma_{\tau\tau}/\Gamma_{had} = 0.048$ and the Monte Carlo simulation, 510 $\tau\tau$ events are expected, and 524 were found. This identification, however, is not used in the analysis.

We are left with a total of 18 470 events. The distribution in total calorimetric energy is shown in Fig. 1a, together with the Monte Carlo prediction. Fig. 1b shows the distribution of the calorimetrically determined thrust axis. The experimental energy distribution is somewhat wider than the simulation. This difference is due to noise problems in the hadron calorimeter but has a negligible effect on the detection efficiency; the only use made here of HCAL is the 20 GeV total calorimetric energy requirement. This conclusion is corroborated by the agreement between data and Monte Carlo at low energy in Fig. 1a. The calculated efficiencies are (99.4 ± 0.2)% for hadronic events, and (60 ± 6) % for $\tau^+\tau^-$ events. The possible contamination by the two photon process ($\gamma\gamma$) is estimated using the sample at the lowest energy, in which this background would be concentrated. We study the cross-section of the data with calorimetric energy between 20 and 35 GeV (330 events) as a function of the beam energy. The Z component must exhibit the resonance characteristics whereas the $\gamma\gamma$ component is almost independent of energy. There is no indication of a $\gamma\gamma$ component. The upper limit for the whole data sample due to $\gamma\gamma$ background is 0.1%. The total systematic uncertainty in the efficiency for this selection is estimated to be 0.6%.

The charged track selection requires at least 5 tracks in the TPC with the sum of the track energies (assuming the pion mass) larger than 10% of the center-of-mass energy. The tracks must have a polar angle above 18.2°. This ensures that at least 6 TPC pad rows are traversed; at least 4 reconstructed coordinates per track are required. The distance of closest approach of the reconstructed tracks from the collision point must be less than 10 cm along the beam and 2 cm transverse to it. Track reconstruction efficiency is ~ 99%. Distributions based on the tracks, such as multiplicity, total energy, sphericity, thrust, etc. are in good agreement [5,7] with hadronization models [8] . For the accepted events, distributions of the total energy and sphericity axis are shown in Fig. 2a and 2b, respectively. The calculated efficiency for $q\bar{q}$ events is (97.5 ± 0.6)%. The background of $\tau^+\tau^-$ events is estimated at (30 ± 10) events, and is subtracted. The background from the two-photon process is calculated to be 15 pb. To check the two-photon contribution, the cross-section for events with track energy between 0.1 E_{CM} and 0.15 E_{CM} is studied as a function of center of mass energy to separate the resonant and non-resonant

contributions. A non-resonant cross-section of (-2 ± 32) pb is found, and (15 ± 15) pb is subtracted from the observed hadronic cross-section. The total systematic uncertainty in the efficiency for the track selected sample is also estimated at 0.6%.

The trigger efficiency is measured by means of the penetrating track trigger, which is entirely independent, and which overlapped in 92% of the events. Events triggered by the penetrating track trigger and missed by the basic trigger correspond to 0.05% of the accepted event sample. Conservatively, the trigger inefficiency is 0.1±0.1% for both event samples.

4. Luminosity detector, acceptance conditions and trigger

Accurate measurement of the luminosity is essential to the precise determination of the peak cross-section, especially because the acceptance for the Z events is very close to unity and the uncertainty correspondingly small. The Bhabha events used to measure the luminosity have a polar angle dependence of $\sin^{-4}\theta/2$; a clear and well understood acceptance at the inner boundary is therefore crucial.

The ALEPH luminosity detector consists of a wire chamber arrangement followed by a calorimeter (LCAL) around the beam pipe at small angles on both sides of the detector. Only the calorimeter is used in the present analysis. It is a 38 layer lead and proportional-wire chamber sandwich construction, read out in projective towers, 784 on each side (see Fig. 3a). Each tower is read out in 3 stories, 4.7, 10.4 and 9.4 radiation lengths in depth, respectively. There are two semicylindrical modules on each side covering the polar angle range 42-160 mrad. Within each module, the mechanical precision in the relative position of the towers is 120 μm. The uncertainty on the inner radius due to the relative positioning of the two modules is 140 μm. The distance of the shower maximum from the collision point is 280 cm. The energy resolution is 3%, tower-to-tower response uniformity ± 2%, and the spatial resolution of the shower position 1.2 mm in x and y.

The acceptance region is defined by a boundary between towers as shown for one half of one module in Fig. 3a. The acceptance region excludes an inner band of towers and further excludes a large outer region, essentially the region outside ~110 mrad. The latter exclusion results in a loss of ~15% of the luminosity events, but was desirable, since this region is shadowed by the end-plate of the ITC and TPC, degrading the electron energies somewhat and consequently introducing a systematic error. Acceptance requires that the electron or positron shower pulse height in the front storey is larger in the acceptance region than in the boundary region on one side. There is no such requirement on the opposite side other than that the shower position be inside a 125 mrad contour. The side on which the boundary conditions must be met alternates from one event to the next. The asymmetry in the acceptance condition, together with

the requirement of alternation from event to event, ensure that the acceptance is independent, in first order, of transverse and longitudinal displacement of the collision point and of small displacements of the beam direction. The pulse height requirement across the fiducial boundary results in a remarkably precise definition of the fiducial region: the position uncertainty at the boundary is ~150 μm. The projective nature of the geometry is essential here. The x - y position of the beam crossing relative to the calorimeters is measured for each LEP fill on the basis of the shower positions on the two sides with a precision of ~ 0.2 mm, but the consequent corrections are negligible.

In addition to the geometric requirement, it is required that the energy on each side is greater than 0.22 E_{CM}, and the sum greater than 0.6 E_{CM}.

Three triggers were used in the luminosity determination:

A basic luminosity trigger. This trigger requires a coincidence between the two sides with more than 20 GeV on one and 16 GeV on the other.

A high level single trigger, requiring more than 31 GeV on either side. This trigger serves as a check and permits the efficiency determination of the basic trigger.

Prescaled single triggers of more than 20 GeV and 16 GeV on either side. These triggers enable determination of the background due to random coincidences of off-momentum electrons.

The initial data sample [5] had a small problem in the coincidence trigger, which has since been corrected. The luminosity trigger inefficiency for the total sample is measured to be $(0.1 \pm 0.1)\%$.

Fig. 3b shows the polar-angle distribution of accepted events on the fiducial side, for data and simulation. Fig. 3c shows the total energy distribution. Fig. 3d shows the distribution in the difference, $\Delta\phi$, between the azimuthal angles in the two arms after correction for beam position and magnetic deflection. The Bhabha events are near 180°; a cut at 170° is applied. The data shown in this figure also permit an estimate of the background due to random coincidences in the two sides between single, off-momentum particles. This background is distributed much more broadly in $\Delta\phi$ than the luminosity events. The events in the region $0° < \Delta\phi < 10°$ and $160° < \Delta\phi < 170°$ can be used to subtract the background at $170° < \Delta\phi < 180°$. As can be seen in Fig. 3d, the background is small, at a level of ~ 0.4%.

The effective cross-section is calculated using an event generator that includes first-order radiative corrections [9]. The events were generated at 91.0 GeV collision energy and the cross-

section is found to be 26.78 ± 0.15 (stat) ± 0.20 (theo) nb at 91.0 GeV. For other energies this cross-section was multiplied by the factor $(91\ \mathrm{GeV}/E_{CM})^2$ and corrected for small (< 1%) electroweak effects.

We checked that the cross-section within our cuts is not very sensitive to radiative corrections. The difference between the lowest-order and the first-order calculations is about 1%. The systematic error introduced by neglecting higher orders is expected to be smaller than this value; we assume an error of 0.7%. The hadronic vacuum polarization has been included [10]. The uncertainty for the small momentum transfer involved is of order 10^{-4}, and is therefore negligible.

The systematic relative errors in the determination of the luminosity are estimated as follows:

Position of pad towers within a module and between the two halves	0.002
Inadequacy of simulation	0.009
Energy resolution and cell to cell variation	0.003
Uncertainty in collision position and beam angle relative to calorimeters	negligible
Theoretical uncertainty, higher order radiative effects	0.007
Statistics of simulation	0.004
Total estimated systematic error	0.013

Some checks on the systematic quality of the luminosity measurements were possible. The precision of the geometrical event selection could be checked by repeating the selection, but basing it not on the first calorimetric layer of 4.7 radiation lengths, but instead on the second of 10.4 radiation lengths which contains the bulk of the shower. In a sub-sample of the data, 4169 events were selected on the basis of the first layer and 4171 on the basis of the second. A total of 6 events were not in common. A second, more comprehensive, check was possible by comparing the result to that obtained on the basis of a more restrictive selection in which the inner boundary is displaced by one tower width. The ratio of accepted events was found to be 0.732 ± 0.004 compared to the Monte Carlo expectation of 0.729. In a third check, the energy requirement was changed from the fraction of 0.6 for the total energy to 0.66 and 0.55 of the beam energy for the showers on the fiducial and non-fiducial sides respectively. The acceptance changed by 1.5 % compared to the Monte Carlo expectation of 1%. The discrepancy of 0.5% is due to known flaws in the detector simulation, but is below the given error of 0.9%.

5. Cross-sections on the Z Resonance

Data were obtained at 11 energies: at the Z peak, and at the peak ± 0.25 GeV, ± 1.0 GeV, $+1.5$ GeV, ± 2.0 GeV, ± 3.0 GeV and $+4.0$ GeV. The results reported here are based on ~ 20 000 Z decays which include the 3 300 already reported [5]. The calorimetric selection did not require the TPC, so that its integrated luminosity is higher than that for the track selection. For the data accessible to both selections, 96% of the events are in common. The remaining 4% are found only calorimetrically: 2/3 of these are $\tau^+\tau^-$ decays and the remaining 1/3 are hadronic decays. These differences are as expected from the simulation. A detailed comparison of the two selections for the events with at least 5 tracks finds an agreement of better than 0.3%.

The number of Z and luminosity events are given in Table 1 for the different energies and the two event selections. The resultant hadronic cross-sections are listed as well. In the case of the track selection, $\sigma_{had} = \frac{N_{track}}{\varepsilon_{track}} \frac{\sigma_{Lum}}{N_{Lum}}$, where $\varepsilon_{track} = 0.975 \pm 0.006$.

In the case of calorimetric selection, $\sigma_{had} = \frac{N_{cal}}{\varepsilon_{cal}} \frac{\sigma_{Lum}}{N_{Lum}}$,

where $\varepsilon_{cal} = \varepsilon_{cal,had} + \frac{\sigma_\tau}{\sigma_{had}} \varepsilon_{cal,\tau}$

$= 0.994 + 0.048 \cdot 0.60 = 1.022 \pm 0.006$ (at the peak),

where the error includes all systematic uncertainties.

In the following analysis, the average result of the two selections, also given in Table 1, is used. The systematic errors are not included in Table 1. They are 1.3% for the luminosity measurement, 0.6% for the Z events of each selection, and 0.4% for the corresponding error in the combined cross-section.

6. The resonance parameters

The energy dependence of the cross-section near the Z resonance is expected to have the Breit-Wigner form:

$$\sigma_{had} = \sigma^0_{had} \frac{s\,\Gamma_z^2}{(s-M_z^2)^2 + s^2\,\Gamma_z^2/M_z^2} \quad (1+\delta_{rad}(s)) \qquad (1)$$

where $\sigma^0_{had} = 12\pi \frac{\Gamma_{ee}\,\Gamma_{had}}{M_z^2\,\Gamma_z^2}$.

Here, Γ_{ee} and Γ_{had} are the partial widths for Z decay to e^+e^- and $q\bar{q}$, respectively, Γ_z is the total Z width, and M_z is the Z mass. To obtain a meaningful cross-section the bremsstrahlung from the

initial state has to be resummed to all orders as described in ref. [11-15]. The effect of these corrections is summarized in the term $\delta_{rad}(E)$ of (1), which, although of the order of 30% at the peak, is known to better than 0.5%.

A three-parameter fit to the data on the basis of equation (1) and the computer program of Burgers [15] and the formula of Borelli et al. [16] yields the peak cross-section σ^o_{had}, the Z mass and Γ_Z:

$$\begin{aligned} \sigma^o_{had} &= 41.4 \pm 0.8 \text{ nb} \\ M_Z &= 91.182 \pm 0.026 \text{ (exp)} \pm 0.030 \text{ (beam) GeV} \\ \Gamma_Z &= 2.541 \pm 0.056 \text{ GeV}. \end{aligned}$$

The beam error in M_Z is due to the uncertainty in the mean e^+e^- collision energy. This error was determined by the LEP Division [17].

The absolute scale error from luminosity and acceptance systematic errors introduces correlations between the points, and these correlations have been taken into account in the fit. In the result for M_Z, the error due to the uncertainty in the collision energy is stated separately. The possible changes in beam energy from one run period to another do not contribute significantly to any of these quantities.

The χ^2 of the fit is 10.5 for 8 degrees of freedom. The cross-sections and the expectations for two, three or four neutrinos are presented in Fig. 4. Fig. 5 shows the 68% and 99% confidence limit contours in the σ^o_{had} - Γ_Z plane. The results are in agreement with, but considerably more precise than, the measurements of only two months ago [1 - 5].

So far this determination of the Z resonance parameters has been essentially model independent. It is possible to use the Standard Model predictions for the partial widths [18],

$$\begin{aligned} \Gamma_{had} &= 1737 \pm 22 \text{ MeV} \\ \Gamma_{l^+l^-} &= 83.5 \pm 0.5 \text{ MeV} \\ \text{and} \quad \Gamma_{\nu\bar{\nu}} &= 166.5 \pm 1.0 \text{ MeV}, \end{aligned}$$

together with $\Gamma_Z = \Gamma_{had} + 3\Gamma_{l^+l^-} + N_\nu \Gamma_{\nu\bar{\nu}}$ to find N_ν on the basis of the measured total width Γ_Z. The result is $N_\nu = 3.30 \pm 0.37$.

7. Number of neutrino families

In the frame of the standard model, the statistically most powerful way to obtain the number of neutrino families is not from the measurement of the width, but from the peak cross-section, σ^0_{had}. The data are refitted with only N_ν and M_Z as parameters. Since the mass determination is independent of the absolute cross-section and the width, M_Z changes only slightly in this fit. We find:

$$M_Z = 91.175 \pm 0.027 \pm 0.030 \text{ GeV}$$

and $$N_\nu = 3.01 \pm 0.15 \text{ (exp)} \pm 0.05 \text{ (theo)}.$$

The theoretical uncertainty is due to uncertainties in the partial width calculation and is discussed in our previous letter [5]. The χ^2 of this fit is 11.3 for 9 degrees of freedom. The agreement with the earlier results [1-5], which give an average of $N_\nu = 3.13 \pm 0.25$, is good.

8. Leptonic branching ratios

The leptonic branching ratio of the Z [19,20] has been determined, using the larger data sample, in a way similar to that reported in [19]. The result of the detailed analysis is given in Table 2. The e^+e^- and $\tau^+\tau^-$ channels were analyzed in a manner identical to [19] using the same range of energies. A somewhat larger data sample, however, was used for the $\tau^+\tau^-$ than for the e^+e^-. For the $\mu^+\mu^-$ channel a slightly different procedure to [19] was adopted in order to extend the angular range to $|\cos\theta| < 0.90$ and data at all center-of-mass energies were used. Candidate events for $\mu^+\mu^-$ pairs were selected as in [19]. However, muons were identified here by requiring also that at least one of the two energetic tracks to have a low energy deposit in the ECAL, compatible with a minimum ionizing particle. Some runs in which the HCAL readout was not operational were excluded. The principal backgrounds in each channel in Table 2 are lepton pairs mistaken as another type of lepton pair. The last row in Table 2 gives the ratios of the numbers of lepton pairs to hadronic events where the latter were selected using the reconstructed charged tracks as described in section 3.

Table 3 shows these ratios (P) together with the branching ratios (B) and partial widths (Γ) deduced from the measured values of σ^0_{had} and Γ_Z derived above, correcting for the effect of single photon exchange. Since the measured leptonic branching ratios are equal within errors, compatible with lepton universality, the average values $\Gamma_{l^+l^-}$, $P_{l^+l^-}$ and $B_{l^+l^-}$ are also given. From these numbers the hadronic and invisible branching ratios are deduced following the procedure described in [19]. They all agree very well with the standard model prediction.

The value of α_s can be checked by using Γ_{had} ; we find $\alpha_s = 0.22 \pm 0.10$, assuming the first order expansion $\Gamma_{had} = \Gamma^0_{had} (1 + \alpha_s / \pi)$.

Since the branching ratios add to unity, the ratio of the invisible to the leptonic width is:

$$\frac{\Gamma_{inv}}{\Gamma_{l^+l^-}} = \frac{1}{B_{l^+l^-}} - \frac{1}{P_{l^+l^-}} - 3 = 5.78 \pm 0.39$$

where $B_{l^+l^-}$ and $P_{l^+l^-}$ are the averaged leptonic branching ratios and the ratio of the leptonic to hadronic events, respectively, and Γ_{inv} and $\Gamma_{l^+l^-}$ are the invisible and leptonic partial widths. Taking the value $\Gamma_{\nu\bar{\nu}}/\Gamma_{l^+l^-} = 1.99 \pm 0.01$, expected from the Standard Electroweak Model, the number of neutrino types is 2.90 ± 0.19. The importance of this result compared to the previous one, to which it is very strongly correlated, is that the ratio $\Gamma_{\nu\bar{\nu}}/\Gamma_{l^+l^-}$ is the only assumption from the standard model used in the analysis. The result is still valid if additional unexpected states yielding hadrons are present in Z decays.

The average leptonic partial width can be related to the effective weak mixing angle $\sin^2\theta_w(M_Z)$ [21] in the following manner:

$$\Gamma_{l^+l^-} = (1 + \kappa) \cdot \frac{\alpha(M_Z) \cdot M_Z \, (1 + (1 - 4 \sin^2\theta_w(M_Z))^2)}{48 \sin^2\theta_w(M_Z) \cos^2\theta_w(M_Z)} \quad ,$$

where $\kappa = (0.2 \pm 0.3) \%$ represents additional electroweak effects [22] and $\alpha(M_Z)$ is the effective QED coupling constant .

From our measurement, $\Gamma_{l^+l^-} = 83.9 \pm 2.2$ MeV, we find:

$$\sin^2\theta_w(M_Z) = 0.231 \pm 0.008.$$

This determination is insensitive to assumptions on the top quark mass, the Higgs boson mass or the Higgs structure of the theory. It constitutes the most precise direct determination at this time of $\sin^2\theta_w$ from neutral current couplings of leptons.

9. Acknowledgements

We would like to thank our colleagues of the LEP division for their outstanding performance in bringing the LEP machine into operation. Thanks also due to the many engineering and technical personnel at CERN and at the home institutes for their contribution towards ALEPH's success. Those of us from non-member states wish to thank CERN for its hospitality.

References

[1] G.S. Abrams et al., Phys. Rev. Lett. 63 (1989) 724;
J.M. Dorfan, MARK II Collaboration, Phys. Rev. Lett. 63 (1989) 2173.

[2] B. Adeva et al. (L3 Collaboration), Phys. Lett. B231 (1989) 509.

[3] M.Z. Akrawy et al. (OPAL Collaboration), Phys. Lett. B231 (1989) 530.

[4] P. Aarnio et al. (DELPHI Collaboration), Phys. Lett. B231 (1989) 539.

[5] D. Decamp et al. (ALEPH Collaboration), Phys. Lett. B231 (1989) 519.

[6] "ALEPH - A detector for electron-positron annihilation at LEP", to be published in Nucl. Instr. Meth.

[7] D. Decamp et al. (ALEPH Collaboration), CERN-EP/89-139, submitted to Phys. Lett.

[8] M. Bengtsson and T. Sjöstrand, Phys. Lett. B185 (1987) 435.

[9] F.A. Berends and R. Kleiss, Nucl. Phys. B228 (1983) 737;
M. Böhm, A. Denner and W. Hollik, Nucl. Phys. B304 (1988) 687;
F.A. Berends, R. Kleiss and W. Hollik, Nucl. Phys. B304, (1988) 712.

[10] H. Burkhardt, F. Jegerlehner, G. Penso and C. Verzegnassi, Z. Phys. C43 (1989) 497.

[11] E.A. Kuraev, V.S. Fadin, Sov.J. Nucl. Phys. 41 (1985) 466.

[12] G. Altarelli, G. Martinelli, in "Physics at LEP", eds. J. Ellis and R. Peccei, CERN 86-02 (1986) Vol I, 47.

[13] F.A. Berends, G. Burgers, W.L. van Neerven, Phys. Lett. B185 (1987) 395.

[14] O. Nicrosini, L. Trentadue, Phys. Lett. B196 (1987) 551.

[15] G. Burgers, in "Polarization at LEP", eds. G. Alexander et al., CERN 86-02 (1986) Vol I, 121.

[16] A. Borelli, M. Consoli, L. Maiani, R. Sisto, CERN TH 5441 (1989).

[17] A. Hofmann, private communication.

[18] F.A. Berends et al in "Z-Physics at LEP I", eds. G. Altarelli, R. Kleiss, C. Verzegnassi CERN 89-08 (1989), Vol. I, 89.

[19] D. Decamp et al. (ALEPH Collaboration), CERN-EP/89-141; to appear in Phys. Lett.

[20] M.Z. Akrawy et al. (OPAL Collaboration), CERN-EP/89-147; to appear in Phys. Lett.

[21] The effective weak mixing angle is defined as the ratio of the running QED and weak coupling constants evaluated at the Z mass:

$$\sin^2\theta_w(M_z) = e^2(M_z) / g^2(M_z) \approx 1 - \frac{M_w^2}{\rho\, M_z^2} .$$

It is defined in different ways in the literature:

- $\sin^2\hat{\theta}_w(M_z)_{\overline{MS}}$: W.J. Marciano and A. Sirlin, Phys. Rev. Lett. 46 (1981) 163;
- $\sin^2\theta_w{}^*(M_z)$ D.C. Kennedy and B.W. Lynn, SLAC Pub 4039 (1986), Nucl. Phys. B322 (1989) 1;
- $\overline{\sin^2\theta_w}$ M. Consoli, W, Hollik, F. Jegerlehner in "Z Physics at LEP 1", eds. G. Altarelli, R. Kleiss, C. Verzegnassi, CERN 89-08 (1989) Vol 1, 7.

The numerical differences are insignificant.

[22] D.C. Kennedy, B.W. Lynn, J.C. Im and R.G. Stuart, Nucl. Phys. B321 (1989) 83.

Table 1

Results for σ_{had} near the Z peak. The number of Z decay candidates and luminosity event numbers and resultant hadronic cross-sections for the two event selections, as well as the combined result are shown. The errors are statistical only.

	Track selection			Calorimeter selection			
Energy GeV	N_{track}	N_{Lum}	Cross-section, nb	N_{cal}	N_{Lum}	Cross-section, nb	Average Cross-section nb
88.278	306	2015	4.43 ± 0.27	405	2447	4.56 ± 0.25	4.49 ± 0.25
89.289	337	1020	9.45 ± 0.59	546	1570	9.46 ± 0.47	9.46 ± 0.47
90.285	1620	2310	19.65 ± 0.63	1714	2341	19.58 ± 0.62	19.61 ± 0.62
91.036	4057	3691	30.16 ± 0.68	4812	4188	30.15 ± 0.64	30.15 ± 0.64
91.288	4312	3835	30.58 ± 0.68	4579	3874	30.82 ± 0.68	30.70 ± 0.68
91.531	2884	2680	29.04 ± 0.78	3501	3136	28.79 ± 0.71	28.92 ± 0.71
92.286	1340	1686	21.01 ± 0.78	1429	1715	21.00 ± 0.76	21.00 ± 0.76
92.565	130	222	15.40 ± 1.71	143	225	15.91 ± 1.73	15.65 ± 1.71
93.292	827	1585	13.50 ± 0.58	913	1685	13.36 ± 0.56	13.43 ± 0.56
94.278	234	688	8.62 ± 0.66	258	715	8.61 ± 0.64	8.61 ± 0.64
95.036	95	396	5.98 ± 0.69	170	662	6.00 ± 0.53	5.99 ± 0.53

Table 2

Details of the evaluation of the corrected number of events for the three channels $Z \to l^+ l^-$. The last row gives the ratio (P) of leptonic events to hadronic events of the same data sample.

	e^+e^-			$\mu^+\mu^-$			$\tau^+\tau^-$		
l^+l^- candidates	398	± 20		382	± 20		581	± 24	
background events	14		± 3	2		± 1	47		± 9
t-channel subtraction	60	± 6	± 5						
$Z \to l^+l^-$ (raw)	323	± 21	± 6	380	± 20	± 1	534	± 24	± 9
Cross-section accept. (%)	73.4			85.5			89.5		
Selection efficiency (%)	94.5		±2.0	96.5		±01.1	91.6		±2.0
Trigger efficiency (%)	100.0	-0.2		98.3	±0.6		99.7	±0.2	
$Z \to l^+l^-$ (corrected)	466	± 30	±13	469	± 25	± 5	653	± 29	±15
Z -> hadrons (corrected)	10385	±103		9769	± 99		13880	±119	
P_l (%)	4.48	±0.30	±0.12	4.80	±0.26	±0.05	4.70	±0.21	±0.11

Table 3

Measured ratios (P) of leptonic to hadronic Z decays, branching ratios (B) and partial widths (Γ) for the different decay modes.

Decay	P	B	Γ(MeV)
$Z \rightarrow e^+ e^-$	0.0448 ± 0.0031	0.0323 ± 0.0012	82.1 ± 3.4
$Z \rightarrow \mu^+ \mu^-$	0.0480 ± 0.0026	0.0346 ± 0.0023	87.9 ± 6.0
$Z \rightarrow \tau^+ \tau^-$	0.0470 ± 0.0024	0.0339 ± 0.0021	86.1 ± 5.6
$Z \rightarrow l^+ l^-$	0.0468 ± 0.0015	0.0330 ± 0.0006	83.9 ± 2.2
$Z \rightarrow$ hadrons		0.710 ± 0.015	1804 ± 44.
$Z \rightarrow$ invisible		0.191 ± 0.014	495 ± 41.

Figure captions

Fig. 1 Distributions for calorimetrically selected events. a) total calorimetric energy; b) absolute value of the cosine of the thrust axis.

Fig. 2 Distributions for track selected events. a) total track energy; b) absolute value of the cosine of the sphericity axis.

Fig. 3 The luminosity calorimeter. a) tower structure in one quadrant showing acceptance boundary; b) distribution of the polar angle. c) distribution of the total Bhabha energy relative to the collision energy, before and after background subtraction. The minimum value for acceptance is 0.6; d) distribution of the difference in the azimuthal angle between the two sides. The acceptance region is $170° < \Delta\phi < 180°$.

Fig. 4 Cross-section for e^+e^- –> hadrons as function of LEP energy. The Standard Model predictions for $N_\nu = 2$, 3 and 4 are shown.

Fig. 5 Contours of constant χ^2 in the σ^o_{had} - Γ_z plane, and the Standard Model predictions for $N_\nu = 2$, 3 and 4.

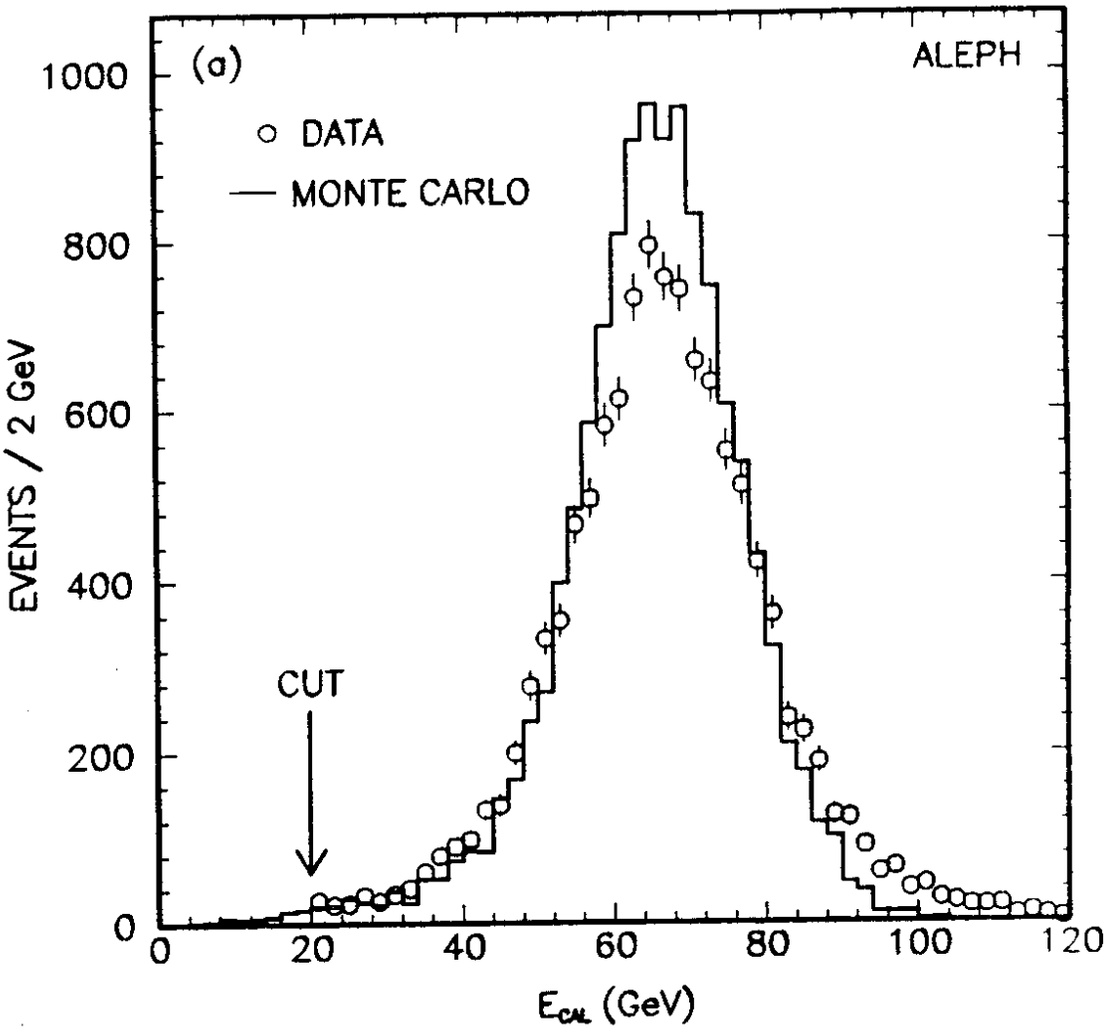
(a)
ALEPH
DATA
MONTE CARLO
CUT
EVENTS / 2 GeV
E_{CAL} (GeV)
0
200
400
600
800
1000
0
20
40
60
80
100
120

Fig. 1a

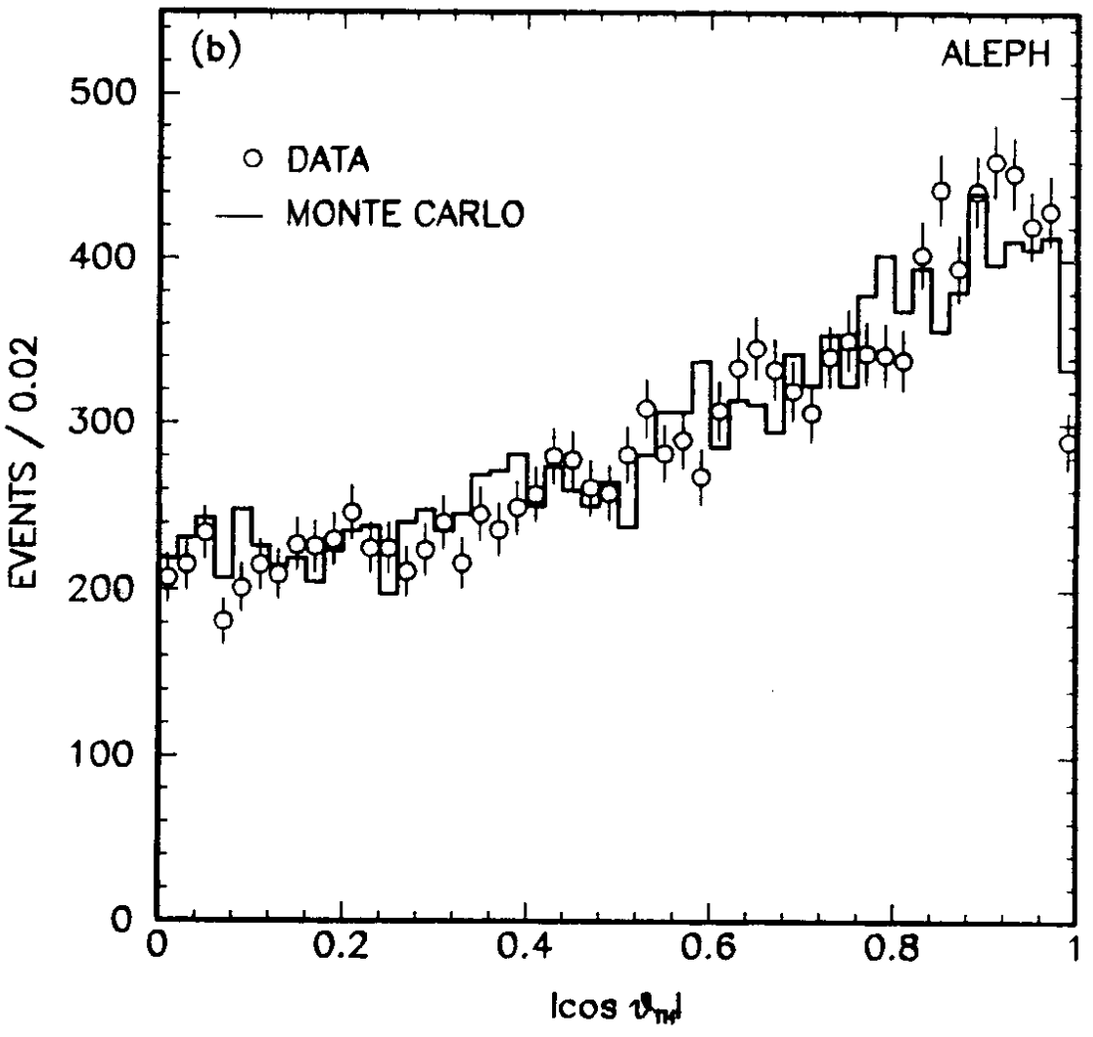
(b)
ALEPH
DATA
MONTE CARLO
EVENTS / 0.02
500
400
300
200
100
0
0
0.2
0.4
0.6
0.8
1
|cos ϑ_thr|

Fig. 1b

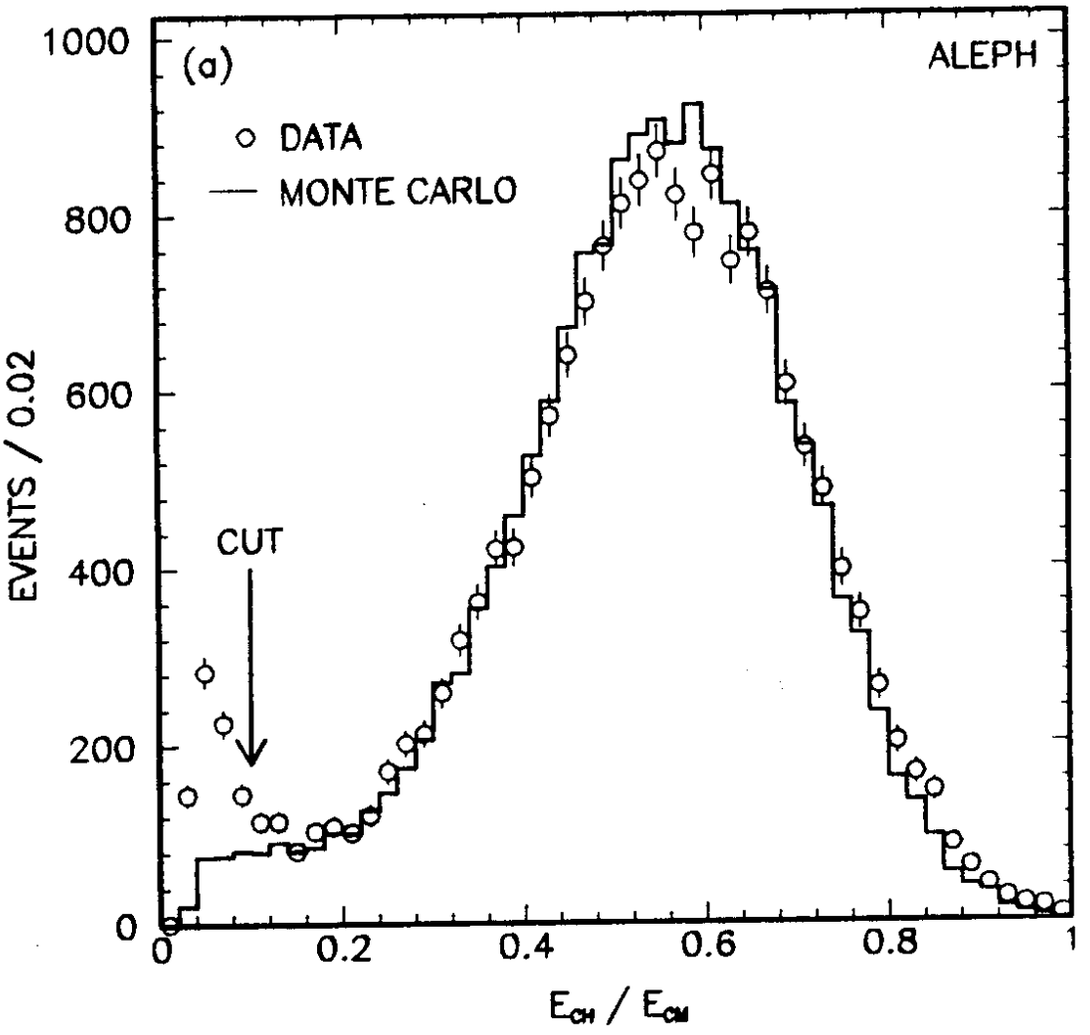
(a)
ALEPH
DATA
MONTE CARLO
CUT
EVENTS / 0.02
1000
800
600
400
200
0
0
0.2
0.4
0.6
0.8
1
E_{CH} / E_{CM}

Fig. 2a

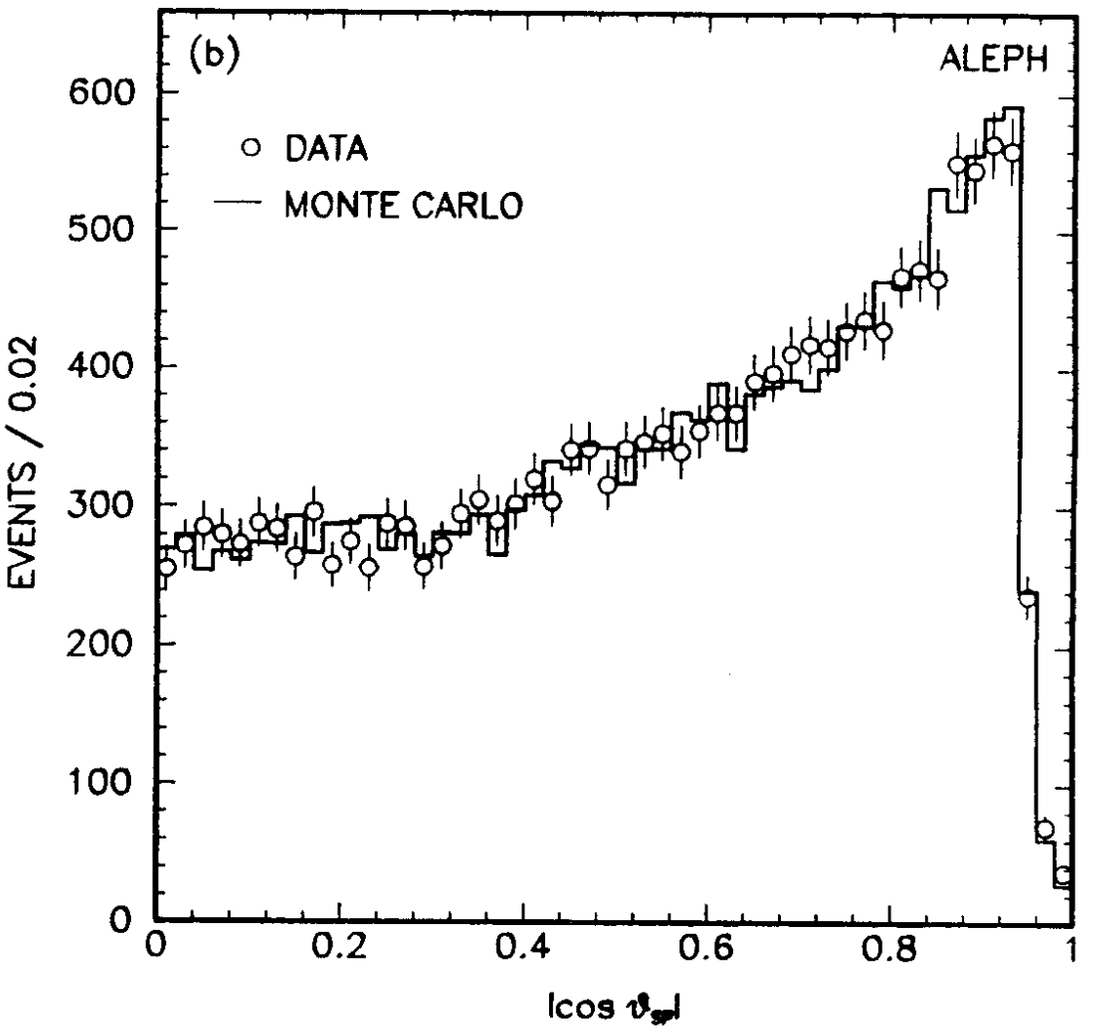
(b)
ALEPH
DATA
MONTE CARLO
EVENTS / 0.02
600
500
400
300
200
100
0
0
0.2
0.4
0.6
0.8
1
|cos ϑ_sph|

Fig. 2b

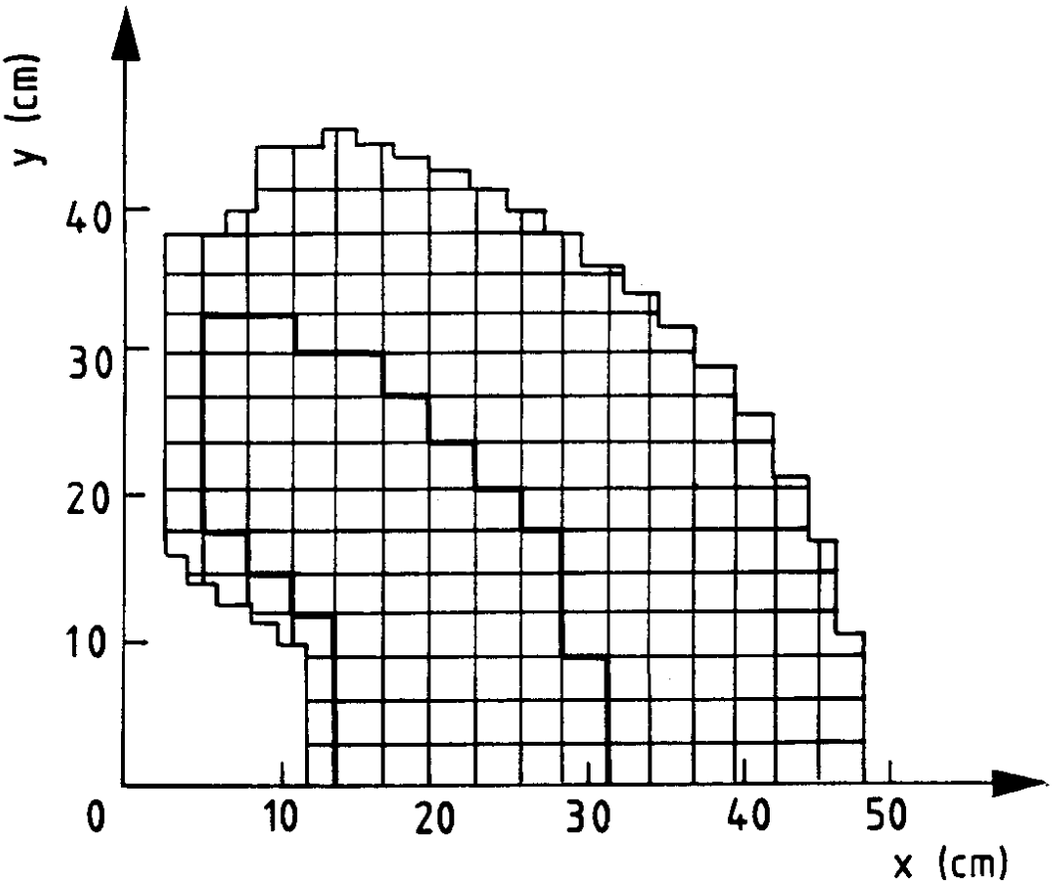

Fig. 3a

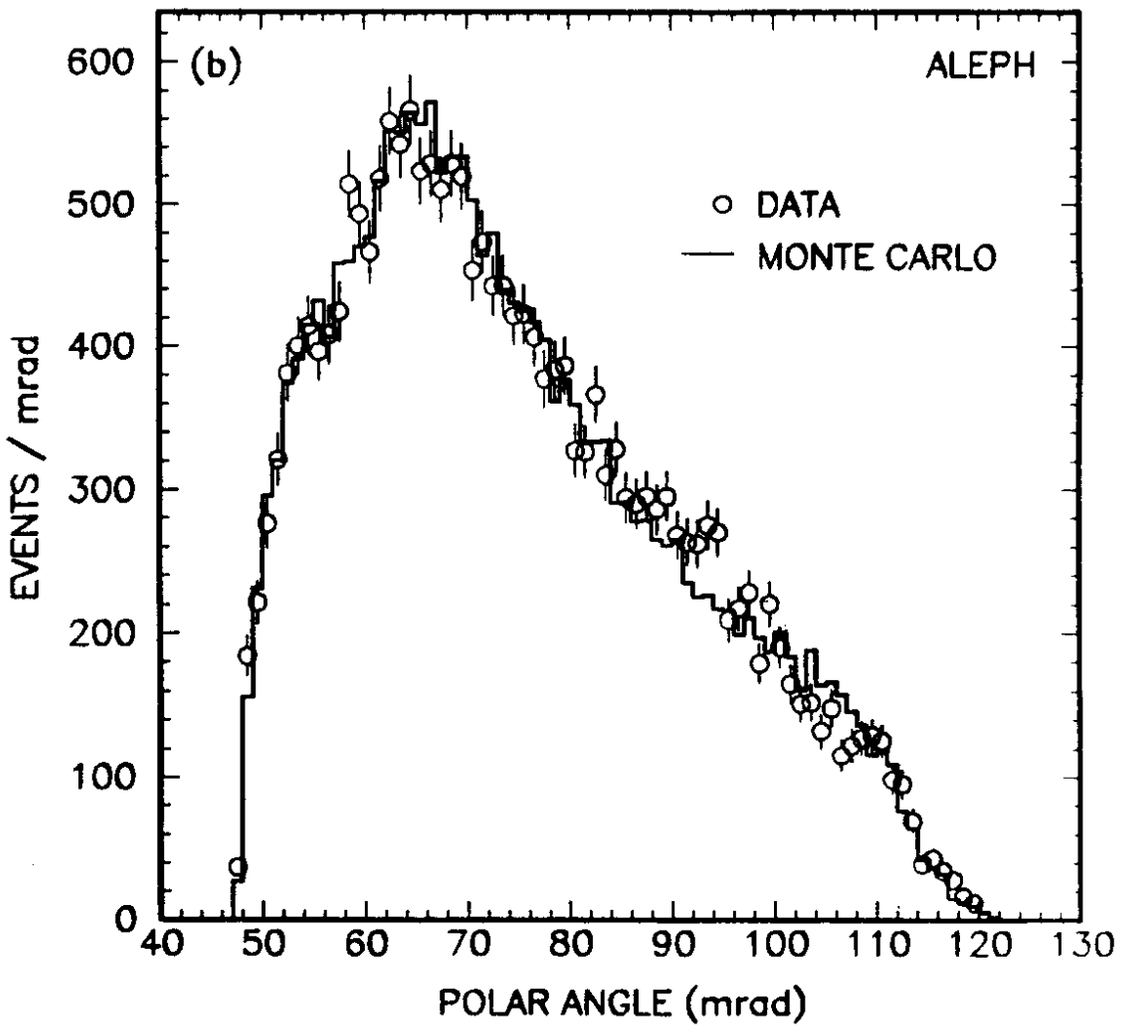
(b)
ALEPH
DATA
MONTE CARLO
EVENTS / mrad
POLAR ANGLE (mrad)
0
100
200
300
400
500
600
40
50
60
70
80
90
100
110
120
130

Fig. 3b

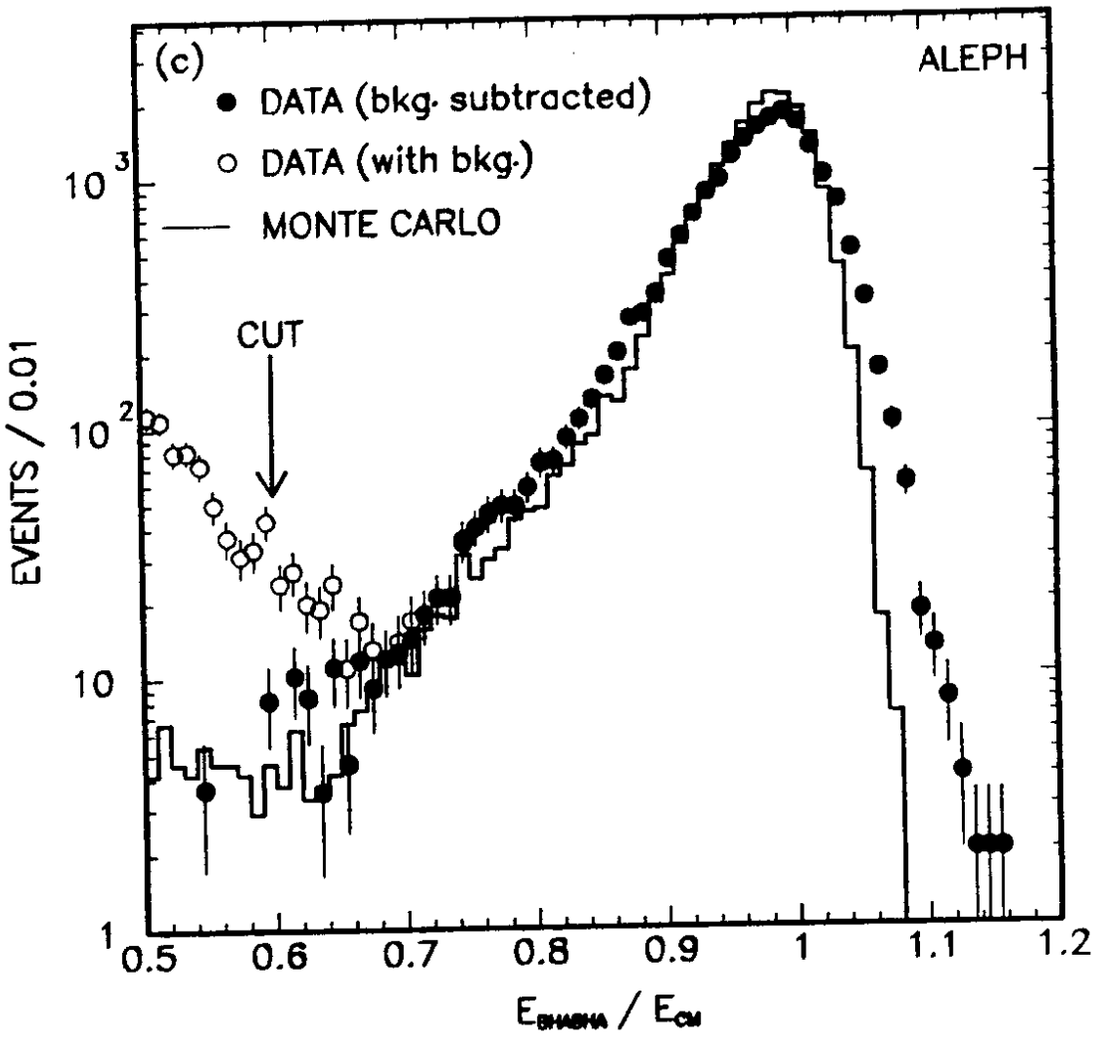
(c)
ALEPH
DATA (bkg. subtracted)
DATA (with bkg.)
MONTE CARLO
CUT
EVENTS / 0.01
10^3
10^2
10
1
0.5
0.6
0.7
0.8
0.9
1
1.1
1.2
E_{BHABHA} / E_{CM}

Fig. 3c

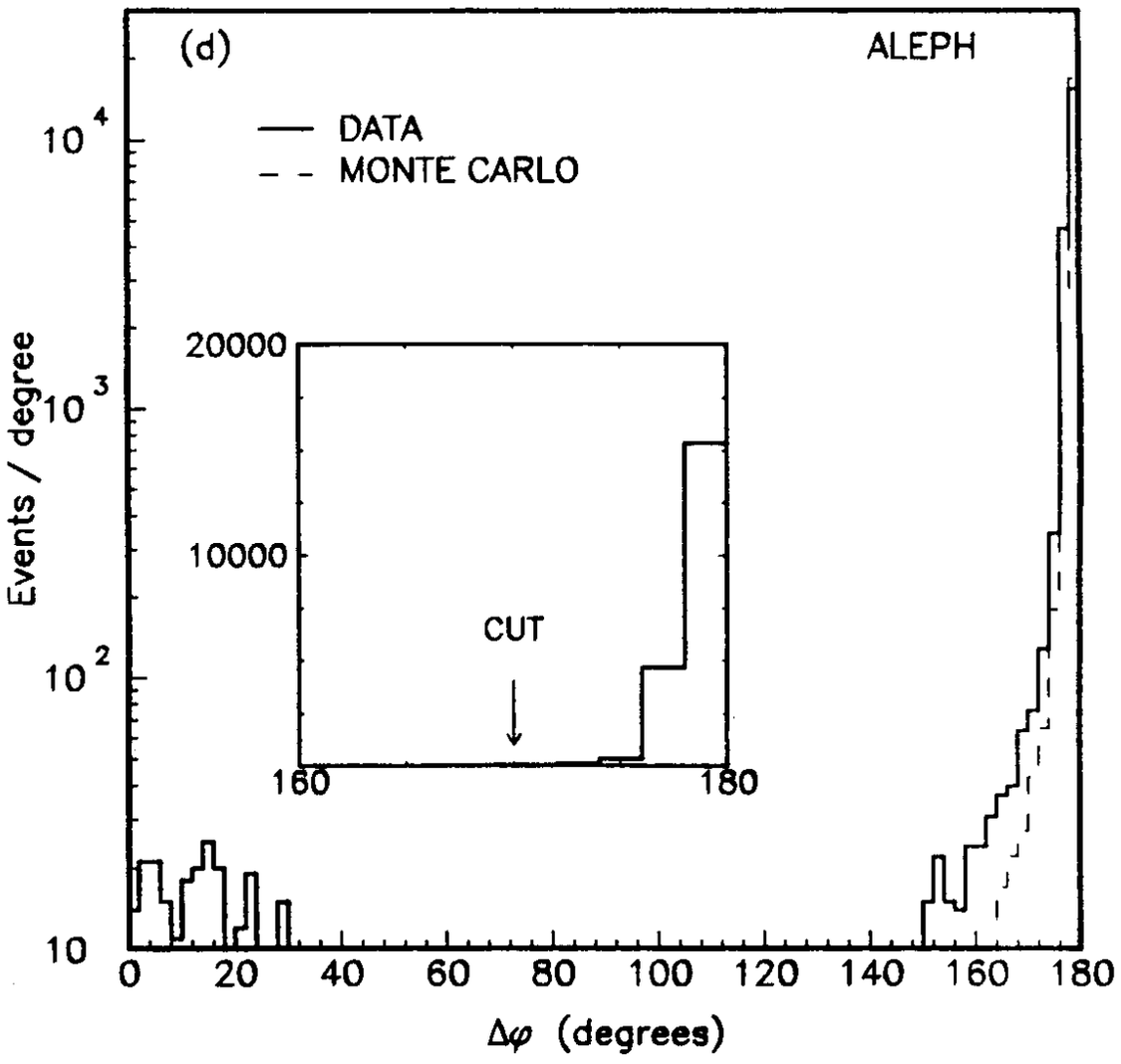
(d)
ALEPH
DATA
MONTE CARLO
Events / degree
10^4
10^3
10^2
10
20000
10000
CUT
160
180
0
20
40
60
80
100
120
140
160
180
Δφ (degrees)

Fig. 3d

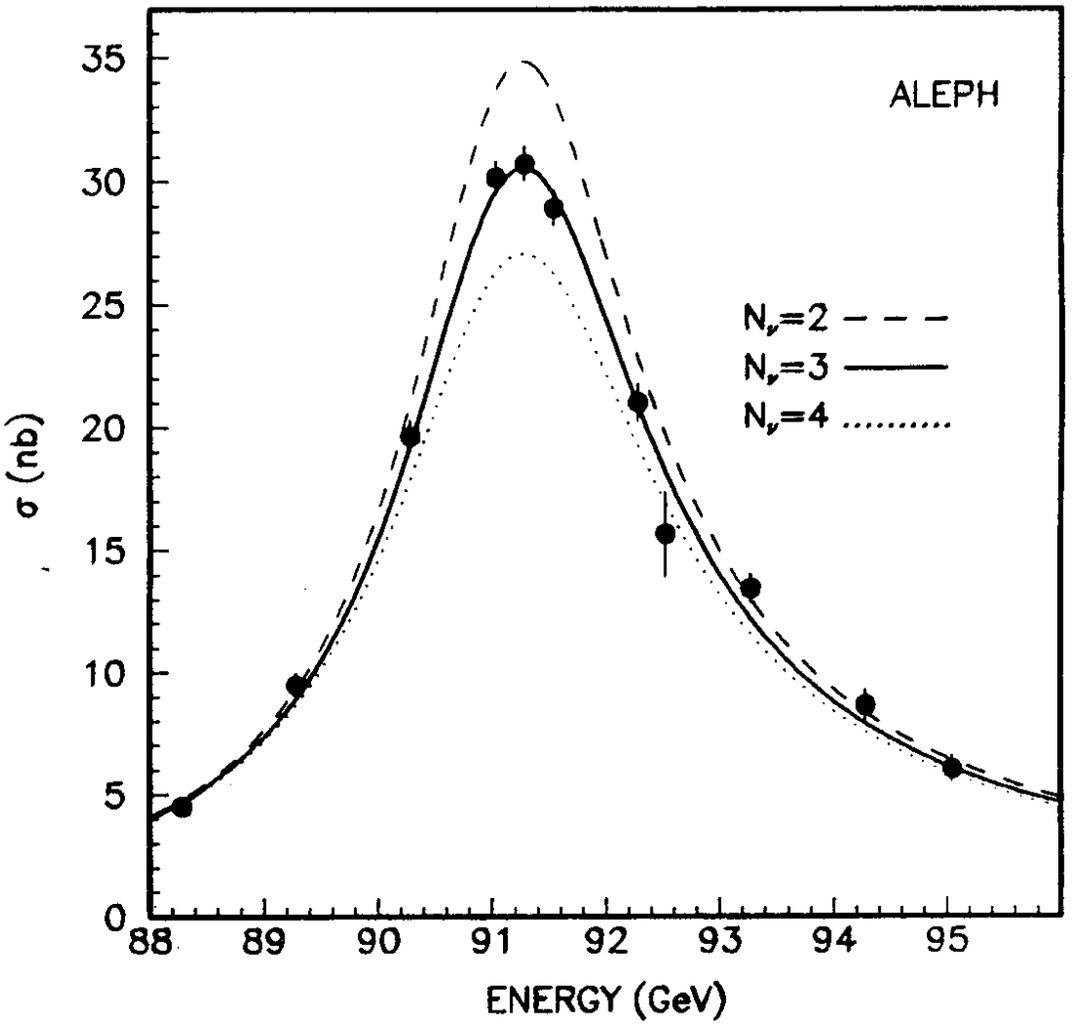
ALEPH
N_ν=2
N_ν=3
N_ν=4
σ (nb)
ENERGY (GeV)
0
5
10
15
20
25
30
35
88
89
90
91
92
93
94
95

Fig. 4

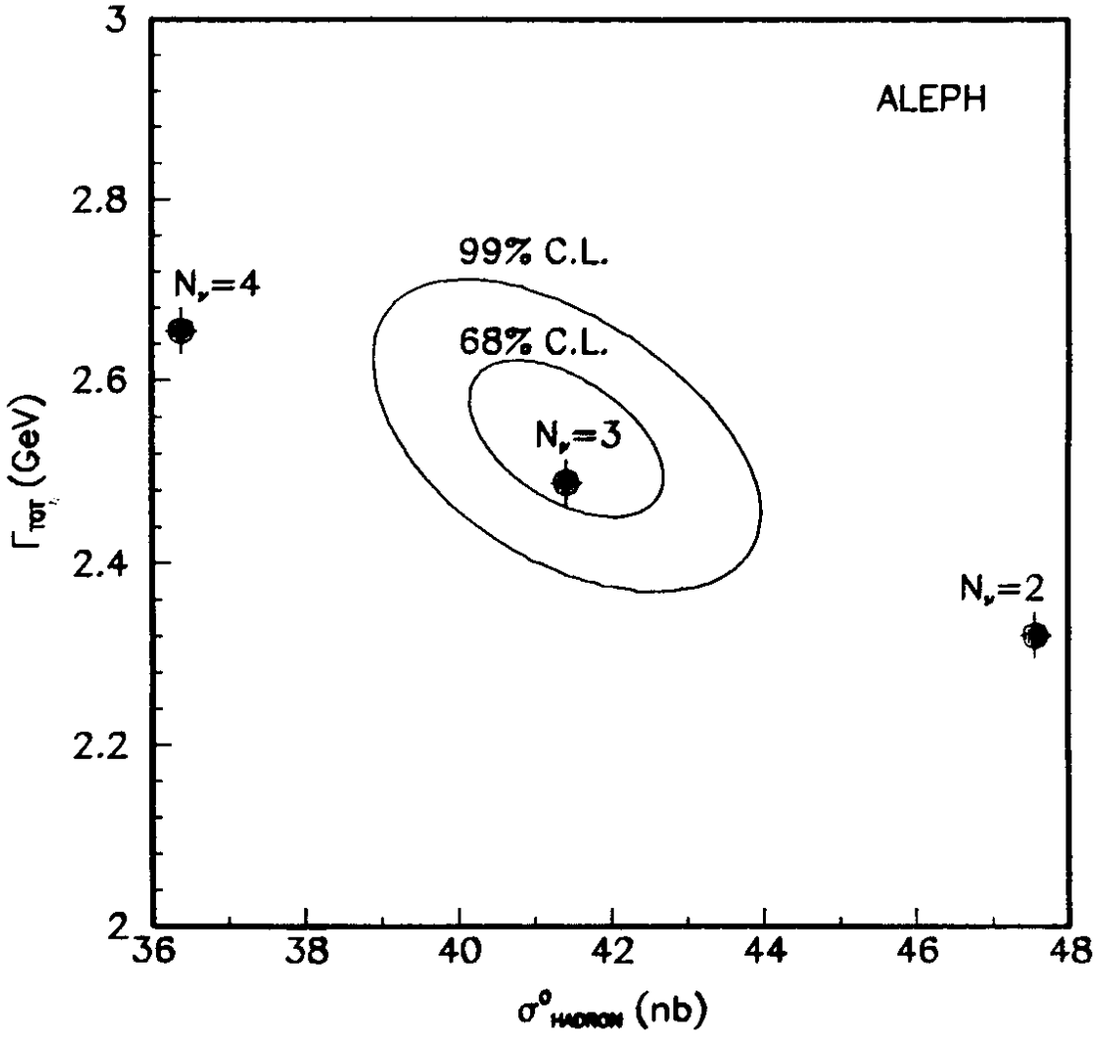
ALEPH
99% C.L.
68% C.L.
N$_\nu$=4
N$_\nu$=3
N$_\nu$=2
Γ_{TOT} (GeV)
σ^0_{HADRON} (nb)
3
2.8
2.6
2.4
2.2
2
36
38
40
42
44
46
48

Fig. 5